Cell proliferation and cell death during whole-body regeneration in the demosponge Halisarca dujardinii

Andrey Lavrov, Nikolai Melnikov, Fyodor V Bolshakov, Daniyal M. Saidov, Emilie Le Goff, Kseniia Skorentseva, Veronika S. Frolova, Alexander V Ereskovsky

FEBS Letters

FEBS PR science publishing t

Cell proliferation and cell death during whole-body regeneration in the demosponge Halisarca dujardinii

Journal:	*FEBS Letters*
Manuscript ID	Draft
Wiley - Manuscript type:	Research Article
Date Submitted by the Author:	n/a
Complete List of Authors:	Lavrov, Andrey; Lomonosov Moscow State University Faculty of Biology, Pertsov White Sea Biological Station Melnikov, Nikolai; Lomonosov Moscow State University Faculty of Biology, Invertebrate Zoology Bolshakov, Fyodor; Lomonosov Moscow State University Faculty of Biology, Pertsov White Sea Biological Station Saidov, Daniyal; Lomonosov Moscow State University Faculty of Biology, General Ecology and Hydrobiology Le Goff, Emilie; Montpellier University, ISEM Skorentseva, Kseniia; FSBIS Koltzov Institute of Developmental Biology of Russian Academy of Sciences Frolova, Veronika; Lomonosov Moscow State University Faculty of Biology, Embryology Ereskovsky, Alexander; FSBIS Koltzov Institute of Developmental Biology of Russian Academy of Sciences; Institut Méditerranéen de Biodiversité et d'Écologie Marine et Continentale
Keywords:	cell reaggregation,, morphallaxis, cell proliferation, cell death, sponges, Porifera, Demospongiae
Abstract:	Sponges (phylum Porifera) are early-branching metazoans demonstrating an outstanding example of the whole-body regeneration, cell reaggregation. During the process, single cells form aggregates capable of progressive development and reconstruction of intact sponges. This study provides the first comprehensive analysis of cell proliferation and cell death during cell reaggregation in a marine demosponge, Halisarca dujardinii. Relatively high proliferative activity occurs at the early and late stages of the reaggregation. However, proliferation seems to be a consequence of intact tissue turnover rather than a prerequisite for aggregate development. The contribution of cell death is limited to a short period during the aggregate epithelization. Overall cell reaggregation in demosponges appears to be morphallactic restorative process relying primarily on cell migration, dedifferentiation, and transdifferentiation.

Note: The following files were submitted by the author for peer review, but cannot be converted to PDF. You must view these files (e.g. movies) online.

Table S3.rar

Cell proliferation and cell death during whole-body regeneration in the demosponge Halisarca dujardinii

Andrey I. Lavrov[1,*], Nikolai P. Melnikov[2], Fyodor V. Bolshakov[1], Daniyal M. Saidov[3], Emilie Le Goff[4], Kseniia V. Skorentseva[5], Veronika S. Frolova[6], Alexander V. Ereskovsky[5,7]

1 – Pertsov White Sea Biological Station, Biological Faculty, Lomonosov Moscow State University, Leninskiye Gory 1-12, Moscow, 119234, Russia.

2 – Dept. Invertebrate Zoology, Biological Faculty, Lomonosov Moscow State University, Leninskiye Gory 1-12, Moscow, 119234, Russia.

3 – Dept. General Ecology and Hydrobiology, Biological Faculty, Lomonosov Moscow State University, Leninskiye Gory 1-12, Moscow, 119234, Russia.

4 – ISEM, Univ Montpellier, CNRS, IRD, Montpellier, France.

5 – Koltzov Institute of Developmental Biology of Russian Academy of Sciences, 26 Vavilov Street, Moscow, 119334, Russia.

6 – Dept. Embryology, Biological Faculty, Lomonosov Moscow State University, Leninskiye Gory 1-12, Moscow, 119234, Russia.

7 – Institut Méditerranéen de Biodiversité et d'Ecologie, Aix Marseille Univ, Avignon Univ, CNRS, IRD, Station Marine d'Endoume, Rue de la Batterie des Lions, 13007, Marseille, France.

** Corresponding author: lavrovai@my.msu.ru*

ORCID and e-mails

AL 0000-0002-0788-9039, lavrovai@my.msu.ru

NM 0000-0002-1154-2556, npmelnikoff@gmail.com

FB 0000-0001-7543-2826, fedbolsh@mail.ru

DS 0000-0003-3954-0170, Daniyalsaidov@yandex.ru

ELG 0000-0002-6658-6927, emilie.le-goff@umontpellier.fr

KS 0000-0002-4222-0517, skorentseva.ksenya.2016@post.bio.msu.ru

VF 0009-0000-8401-3367, frolova.veronika.2014@post.bio.msu.ru

AE 0000-0003-1079-7204, alexander.ereskovsky@imbe.fr

ABSTRACT

Sponges (phylum Porifera) are early-branching metazoans demonstrating an outstanding example of the whole-body regeneration, cell reaggregation. During the process, single cells form aggregates capable of progressive development and reconstruction of intact sponges. This study provides the first comprehensive analysis of cell proliferation and cell death during cell reaggregation in a marine demosponge, *Halisarca dujardinii*. Relatively high proliferative activity occurs at the early and late stages of the reaggregation. However, proliferation seems to be a consequence of intact tissue turnover rather than a prerequisite for aggregate development. The contribution of cell death is limited to a short period during the aggregate epithelization. Overall cell reaggregation in demosponges appears to be morphallactic restorative process relying primarily on cell migration, dedifferentiation, and transdifferentiation.

Key words: cell reaggregation, morphallaxis, cell proliferation, cell death, sponges, Porifera, Demospongiae

INTRODUCTION

Whole-body regeneration (WBR) represents the most radical case of reparative regeneration in animals implying a complete restoration of the body from its small fragment. WBR has limited phylogenetic distribution, and most of its examples are associated with early-branching metazoans: sponges (Ereskovsky *et al.*, 2021), placozoans (Kuznetsov *et al.*, 2022; Osigus *et al.*, 2022), ctenophores (Edgar *et al.*, 2021), and cnidarians (Seybold *et al.*, 2016; Kirillova *et al.*, 2018). However, WBR is also known in acoels (Srivastava *et al.*, 2014), planarians (Ivankovic *et al.*, 2019; Vila-Farré *et al.*, 2023), annelids (Kolbasova *et al.*, 2014; Kostyuchenko and Kozin, 2021), mollusks (Mitoh and Yusa, 2021), echinoderms (Cary *et al.*, 2019; Carnevali *et al.*, 2024), and tunicates (Brown *et al.*, 2009; Blanchoud *et al.*, 2018).

Sponges (phylum Porifera) are early-branching metazoans with unique anatomical organization and tissue composition (Ereskovsky and Lavrov, 2021). Sponge tissues and cell types show high plasticity that lies at the core of their pronounced regenerative abilities: these animals can regenerate not only small wounds (Borisenko *et al.*, 2015; Ereskovsky *et al.*, 2015, 2020; Lavrov *et al.*, 2018; Skorentseva *et al.*, 2023) but also show wide array of WBR types (Ereskovsky *et al.*, 2021; Riesgo *et al.*, 2022). Moreover, sponges demonstrate one of the most outstanding examples of WBR across Metazoa – the process of cell reaggregation. In the course of the restorative process, sponges can reconstruct intact organization from a suspension of single cells: after dissociation, single cells coalesce into multicellular aggregates, which retain viability and are capable of progressive development ending with the reconstruction of intact sponges (Lavrov and Kosevich, 2014; Eerkes-Medrano *et al.*, 2015). Cell reaggregation represents a promising model system for studying tissue integration in animals. The whole process of tissue re-establishment can be analyzed under controlled conditions including observations of cell behavior and migration, functional experiments, *etc.* The first essential step in elaborating of such a model system is the description of the normal development of multicellular aggregates and the morphogenetic mechanisms underlying it.

In vivo, histological and ultrastructural studies have shown that sponge cell reaggregation and subsequent aggregate development occur due to active cell migrations, massive cell dedifferentiations and transdifferentiations (Lavrov and Kosevich, 2014, 2016; Eerkes-Medrano *et al.*, 2015; Ereskovsky *et al.*, 2016). RNA-seq studies of cell reaggregation render this process highly dynamic with thousands of genes changing their expression, including transcription factors, pluripotency markers, members of major signaling pathways, *etc* (Soubigou *et al.*, 2020; Borisenko *et al.*, 2021, 2022). Despite the important morphogenetic role of cell proliferation and cell death in various regenerative processes of metazoans, they remain almost unstudied in the

context of sponge cell reaggregation.

In the current study, we have qualitatively and quantitatively described cell proliferation and cell death at the main stages of cell reaggregation in marine demosponge *Halisarca dujardinii* Johnston, 1842. Cell proliferation takes place during the early and late stages of cell reaggregation, while the intermediate stages of epithelized primmorphs contain almost no cycling cells. We suppose that the proliferation at the early stages of reaggregation is maintained mostly by cells involved in the regular renewal of intact tissues (i.e., by cells finishing already started cell cycle), while the proliferation at the late stages of reaggregation reflects the re-entering of cells into the proliferative state due to the reconstruction of intact tissues with their homeostatic turnover. Contrary to cell proliferation, cell death is upregulated during the reaggregation, showing a single peak during the transformation of primary aggregates into the epithelized primmorphs. While the precise morphogenetic role of this upregulation remains unclear, it could indicate some sorting of viable cells required for further development.

MATERIALS AND METHODS

Material collection and cell reaggregation experiments

Specimens of *Halisarca dujardinii* Johnston, 1842 (Fig. 1A) were collected in Kandalaksha Bay of the White Sea in the environs of the Pertsov White Sea Biological Station (66º34' N, 33º08'E) from the upper subtidal zone at 0–2 m depth at low tide. Before the experiments, the sponges were maintained in a 100 L laboratory aquarium with natural seawater and biological filters at 8–12ºC for no longer than 24 hours.

A total of 31 individuals were used in the experiments. The experiments were conducted over four years (2017-2021) in the second half of August and September, when *H. dujardinii* is at the stage of post-reproductional growth optimal for cell reaggregation (Lavrov *et al.*, 2020).

Sponge tissues were dissociated by squeezing through 50 µm nylon mesh into vessels with fresh sterile seawater (FSW). The FSW was used in the dissociation procedure and during subsequent cell cultivation to avoid additional contamination. The water was sterilized with 0.22-µm filter units (Corning).

A hemocytometer was used to determine cell concentration in the obtained suspensions. Subsequently, the cell suspensions were diluted with FSW up to concentrations $0.5–3\times10^7$ cells/mL. As previously shown, such variations in the cell concentration do not affect the course and the rate of cell reaggregation in *H. dujardinii* (Lavrov and Kosevich, 2016; Lavrov *et al.*, 2020).

A total of 5 mL of cell suspension was cultured in an individual 30 mm plastic Petri dish. The cell cultures were maintained in FSW at 8–12°C. Half of the culture medium was replaced

with fresh FSW every 48 hours. Each cell culture was checked and photographed daily throughout the cultivation period using the Leica M165FC stereomicroscope (Leica) equipped with digital camera Leica DFC 320 and the application Leica LAS Store and Recall v.4.2. The viability of aggregates was evaluated on the basis of their general morphology.

Histological studies

Intact tissues and multicellular aggregates at main developmental stages were fixed with 2.5% glutaraldehyde (Electron Microscopy Science) supplemented with 0.1% ruthenium red (Sigma-Aldrich) in modified 0.1 M Na-cacodylate buffer (0.1 M Na-cacodylate, 85.55 mM NaCl, 5 mM $CaCl_2$, 5 mM $MgCl_2$; pH 7.0-7.5) for 2 h at 4 ºC and post-fixed with 1% OsO_4 (Electron Microscopy Science) supplemented with 0.1% ruthenium red in the same buffer for 3 h at room temperature (RT) (Lavrov *et al.*, 2022; Lavrov and Ereskovsky, 2022). Between fixation and post-fixation, the specimens were rinsed three times with modified 0.1 M Na-cacodylate buffer for 30 min each time at RT with constant orbital shaking at 70 rpm. After post-fixation, the specimens were dehydrated in ethanol and acetone series and embedded in Epon/Araldite epoxy embedding media (Electron Microscopy Science). Semi-thin sections (1 µm in thickness) were cut on an Ultramicrotome PowerTome XL (RMC Boeckeler) equipped with a 'Diamond' 45° diamond knife. Semi-thin sections were stained with toluidine blue and observed using a Leica DMBL light microscope (LM) equipped with the Evolution LC color photo capture system.

Cell proliferation studies

Two markers were used to study cell proliferation. 5-Ethynyl-2′-deoxyuridine (EdU) (Lumiprobe) was used to label DNA-synthesizing cells (S-phase cells); polyclonal anti-Ser10-phospho-histone H3 antibodies (Sigma-Aldrich H0412) were used to label mitotic cells (late G2-/M-phase). The EdU stock solution (10 mM) was prepared in DMSO (MP Biomedicals).

Cell proliferation was studied at eight stages of cell reaggregation: primary multicellular aggregates (PMA), 1 day post-dissociation (dpd); early-staged primmorphs (ESP), 2 dpd; true primmorphs (TP), 4 dpd; primmorphs with developing aquiferous system, early stages (EAS); primmorphs with developing aquiferous system, intermediate stages (IAS); primmorphs with developing aquiferous system, late stages (LAS); primmorphs with oscular tube rudiments (OTR); reconstructed sponges (RS). Due to the natural variations in the rate of aggregate development, the onset time for the EAS, IAS, LAS, OTR, and RS stages differs between cultures (Table S1).

Cultures obtained from 23 sponges were used for cell proliferation studies. A total of 249 aggregates (13-52 aggregates per reaggregation stage) were studied; each stage was represented by at least two cultures from different individuals (Table S1). For cell proliferation studies, aggregates were transferred from a culture to a new Petri dish with 5 ml of fresh FSW

supplemented with 100 μM EdU and maintained in the medium for 24 h. Aggregates incubated in FSW supplemented with DMSO were used as a negative control. During incubation, the aggregates were cultivated at 8–12°C.

After incubation, the aggregates were fixed with 4% PFA (Sigma-Aldrich) in PBS (Amresco) at 4°C and stored in it from several days to several months prior to further treatments. The fixed aggregates were rinsed three times with PBS for 30 min and incubated three times in Blocking Solution (BS) (1% BSA (MP Biomedicals), 0.1% gelatin from cold water fish skin (Sigma-Aldrich), 0.5% Triton X-100 (Sigma-Aldrich), 0.05% Tween 20 (Sigma-Aldrich) in PBS) for 30 min. Then, EdU was visualized by copper click-chemistry in the following mixture: 4 мМ $CuSO_4$ (ChimMed), 20 mg/ml Sodium L-ascorbate (Sigma-Aldrich), and 10 μM Sulfo-Cyanine3 Azide (Lumiprobe) in PBS. Afterward, the aggregates were rinsed three times with BS for several hours and incubated in the primary antibodies: polyclonal anti-Ser10-phospho-histone H3 antibodies produced in rabbit (1:500) (Sigma-Aldrich H0412) and monoclonal anti-acetylated-α-tubulin antibody produced in mouse, clone 6-11B-1 (1:1000) (Sigma-Aldrich) overnight at 4°C. The aggregates were again rinsed three times with BS for several hours and incubated in the secondary antibodies: Donkey Anti-rabbit IgG Alexa 647 (1:2000; final concentration 0.5 μg/ml) (Thermo Fisher Scientific) and Donkey Anti-mouse IgG Alexa 488 (1:2000; final concentration 0.5 μg/ml) (Thermo Fisher Scientific) overnight at 4°C. The aggregates were then rinsed several times with PBS, and the nuclei were visualized by staining with 2 μg/ml 4′,6-diamidino-2-phenylindole (DAPI) (Acros) or Hoechst 33342 (Sigma-Aldrich) for 2 h.

The stained specimens were rinsed several times with PBS and infiltrated with 30%–60%–90% glycerol-PBS / 2.5% 1,4-diazabicyclo[2.2.2]octane (DABCO) (Sigma-Aldrich) and mounted in 90% glycerol-PBS / 2.5% DABCO. Preparations were studied with CLSMs Nikon A1 (Nikon) or Olympus Fluoview FV10 (Olympus) using lasers with wavelength of 405 nm (DAPI), 488 nm (anti-acetylated-α-tubulin ABI + DAM IgG Alexa Fluor 488 ABII), 561 nm (EdU + Sulfo-Cyanine3 Azide) and 637 nm (anti-Ser10-phospho-histone H3 ABI + DAM IgG Alexa Fluor 647 ABII) wavelengths. The obtained Z-stacks (one per each aggregate) were 40-60 μm thick with 1 μm Z-step.

To evaluate the number of DNA-synthesizing cells in intact sponge tissues, sponges (n=15) were incubated in 100 μM EdU for 24 h, pre-fixed with ice-cold methanol for 5 min and fixed in 4% PFA PBS. Fixed sponges were treated as described above. The obtained Z-stacks (up to three per sponge) were 30-60 μm thick with 1 μm Z-step. Data on mitotic activity in intact tissues of *H. dujardinii* (n=17) were taken from a previously published dataset (Melnikov and Lavrov, 2024a).

Cell death studies

Terminal deoxynucleotidyl transferase dUTP nick end labeling (TUNEL) assay was used to label cell death. Apoptosis was studied at the seven stages of cell reaggregation: ESP (1 dpd), TP (3 dpd), EAS, IAS, LAS, OTR, and RS. Due to the natural variations in the rate of aggregate development, the onset time for the EAS, IAS, LAS, OTR, and RS stages differed between cultures (Table S2).

Cultures obtained from 12 sponges were used for apoptosis studies. Six cultures were used for the TUNEL assay optimization (data not shown) and six cultures were used directly for studies of apoptosis during cell reaggregation. A total of 94 aggregates (5-23 aggregates per reaggregation stage) were studied; fewer aggregates of later stages were studied as they show low apoptosis intensity (Table S2).

Aggregates were fixed with 4% PFA (Sigma-Aldrich) in PBS (Amresco) at 4°C and stored in it for two months prior to further treatments. The fixed aggregates were rinsed three times with PBS for 30 min and permeabilized three times with 0.5% Triton X-100 (Sigma-Aldrich) in PBS for 30 min. Afterward, the aggregates were incubated twice in TdT buffer (New England Biolabs) for 30 min, and the TdT reaction was performed overnight at RT in the following mixture: 0.25 mM $CoCl_2$ (New England Biolabs), 80 units of terminal transferase (New England Biolabs), 20 µM EdUTP (Jena Bioscience) in TdT buffer (New England Biolabs). The aggregates were then rinsed once with PBS, incubated three times in BS for 30 min, and EdUTP was visualized by copper click-chemistry in the following mixture: 4 мM $CuSO_4$ (ChimMed), 20 mg/ml Sodium L-ascorbate (Sigma-Aldrich) and 10 µM Sulfo-Cyanine3 Azide (Lumiprobe) in PBS. After click-reaction, the aggregates were rinsed several times with PBS, and the nuclei were visualized by staining with 2 µg/ml 4′,6-diamidino-2-phenylindole (DAPI) (Acros) for 2 h.

Aggregates for positive control were incubated in DNAse I (Thermo Fisher) at 37°C for 1 h prior to TdT buffer incubation. Aggregates for negative control were incubated in a TdT mixture without the terminal transferase. Otherwise, the control aggregates were treated identically to the experimental ones.

Stained specimens were rinsed several times with PBS and infiltrated with 30%–60%–90% glycerol-PBS / 2.5% DABCO (Sigma-Aldrich) and mounted in 90% glycerol-PBS / 2.5% DABCO. Specimens were studied with a CLSM Nikon A1 (Nikon) using lasers with wavelengths of 405 nm (DAPI) and 561 nm (EdUTP + Sulfo-Cyanine3 Azide). The obtained Z-stacks (one per aggregate) were 40-60 µm thick with 1 µm Z-step.

Data on apoptosis in intact sponge tissues were obtained from intact individuals (n=5) fixed and treated as described above. The obtained Z-stacks (up to three per sponge) were 20-40 µm

thick with 1 μm Z-step.

Quantitative and statistical analysis

The quantification of proliferating and apoptotic cells was performed in Bitplane Imaris v9.9.0. Nuclei stained with DAPI, EdU, pH3, or TUNEL were marked and counted with the "Spots" tool, combining automatic counting via Quality thresholds with subsequent manual correction. Based on these data, the proportions of EdU+ cells, pH3+ cells, and TUNEL+ cells were estimated for each observation (Table S3). Subsequently, the mean value and 99% bootstrap confidence interval (CI) were calculated for these parameters. The values reported in the text are means with 99% CI lower and upper limits. To evaluate differences in the parameters between intact tissues and reaggregation stages, Welch's ANOVA with the pairwise Games-Howell post-hoc analysis was conducted. The significance level was 0.01. The p-values reported in the text are Games-Howell p-values. Statistical analysis was performed in R Statistical Software (v4.2.2; R Core Team, 2022) with the basic package "stats" ver. 4.2.2 (R Core Team, 2022) and additional packages "rstatix" ver. 0.7.2 (Kassambara, 2023), "boot" ver. 1.3-28 (Davidson, Hinkle, 1997; Canty, Riple, 2021) and "ggplot2" ver. 3.4.0 (Wickham, 2016).

RESULTS

Stages of cell reaggregation

Cell reaggregation represents a complex developmental process during which an intact sponge is reconstructed from a suspension of single cells. Detailed descriptions of this process in *Halisarca dujardinii*, including the rate of the process, the histology and ultrastructure of multicellular aggregates, cell fate and behavior, were previously reported (Lavrov and Kosevich, 2016; Lavrov *et al.*, 2020; Borisenko *et al.*, 2021). Here we briefly outline the characteristics of the main developmental stages of multicellular aggregates:

1) Primary multicellular aggregates (PMAs), 0-24 hours post-dissociation (hpd). PMAs represent the earliest stage of cell coalescence in a culture (Fig. 2A). They have irregular shapes, rough surfaces, and no obvious internal structure. PMAs are a simple intermix of dedifferentiated cells from a suspension (Fig. 2B).
2) Early-staged primmorphs (ESPs) and true primmorphs (TPs) (Fig. 2C), 1-3 days post-dissociation (dpd). Around 1 dpd PMAs start to transform into ESPs; during the transformation, the surface of the aggregates becomes gradually covered by newly formed exopinacocytes. Exopinacocytes arise through the transdifferentiation of surface cells. ESPs are characterized by forming yet not stable exopinacoderm; TPs, in contrast, have fully formed exopinacoderm, and isolation of the internal milieu of aggregates

occurs at this stage (Fig. 2D). Due to the variations in the rate of exopinacoderm formation, cultures after 1 dpd represent the intermix of ESPs and TPs; around 3 dpd, the exopinacoderm formation is finished in the majority of the aggregates, and cultures predominantly contain TPs.

The subsequent progressive development of TPs starts after a lag phase from one to several days depending on the culture. Progressive development manifests itself in the gradual formation of the aquiferous system, ending with the appearance of one or several oscular tubes.

3) Primmorphs with developing aquiferous system, early stages (EAS), 5+ dpd. The first morphologically visible developmental processes in the inner parts of aggregates start at this stage. At EAS, the development of the new aquiferous system begins with the formation of small cavities throughout the inner cell mass (Fig. 2E, F).
4) Primmorphs with developing aquiferous system, intermediate stages (IAS), 7+ dpd. At this stage, the cavities of the future aquiferous system grow larger, and the development of choanocyte chambers begins through the formation of small dense cell conglomerates in the inner parts of the primmorphs.
5) Primmorphs with developing aquiferous system, late stages (LAS), 9+ dpd. At this stage, the cavities reach their final size and obtain endopinacocyte lining, thus representing functional channels of the aquiferous system (Fig. 2G, H). The rudiments of the choanocyte chambers grow in number and size but usually lack lumen. The number of free cells in the mesohyl decreases, and the fibrillar extracellular matrix becomes evident.
6) Primmorphs with oscular tube rudiments (OTR), 18+ dpd. At this stage, developing primmorphs obtain one or several rudiments of the oscular tubes, which look like blind outgrowths (Fig. 2I). Additionally, ostia appear in the exopinacoderm. In the inner parts, the OTR aggregates contain a fully formed aquiferous system and mesohyl.
7) Reconstructed sponge (RS), 18+ dpd. At this stage, the development of aggregates essentially ends: small fully functional sponges start to pump water through a newly formed aquiferous system (Fig. 2J, K).

The pattern of cell proliferation significantly changes during cell reaggregation

Intact tissues of *H. dujardinii* contain a relatively high number of proliferative cells: 9.98 % (8.20 – 11.96 %) of cells are EdU+ (cells in S-phase) and 0.22 % (0.1 – 0.39 %) of cells are pH3+ (cells in late G2-/M-phase) (Figs. 3A, B, S1; Table 1). Most proliferative cells are choanocytes and reside in the choanocyte chambers (approximately >90%; Melnikov *et al.*, 2022) while cycling

cells in the mesohyl are rare (Fig. 1B, C).

Cell reaggregation in *H. dujardinii* is accompanied by significant changes in the number and distribution of proliferative cells (Figs. 3, 4). Mainly, these changes involve S-phase (EdU+) cells. At the earliest stage of cell reaggregation, in PMAs, the number of EdU+ cells, 6.45 % (4.82 – 8.02 %), does not significantly change in comparison with intact tissues (p-value$_{it\text{-}pma}$ = 0.028) (Fig. 3A; Table 1; Table S3). However, as PMAs represent an intermix of cells from suspension and have no obvious structure, proliferative cells are diffusely distributed (Fig. 4A), in contrast to intact tissues where the majority of proliferative cells are located in choanocyte chambers (Fig. 1C). Some EdU+ cells in PMAs bear flagella indicating their choanocytic origin (Fig. 4A).

During the transformation of PMAs into ESPs, proliferative cells retain diffusive distribution (Fig. 4B) yet their number decreases significantly in comparison with PMAs (p-value$_{pma\text{-}esp}$=5.52×10^{-5}; Table S3): ESPs contain only 2.15 % (1.26 – 3.12 %) EdU+ cells (Fig. 3A; Table 1). These changes become more evident during the further transformation of ESPs into TPs: the number of EdU+ cells decreases even further (p-value$_{esp\text{-}tp}$=5.46×10^{-4}; Table S3), and TPs contain almost no EdU+ cells, 0.24 % (0 – 0.57 %) (Fig. 4C; Fig 3A; Table 1).

The number of EdU+ cells persists at a low level during early stages of aquiferous system development (at the EAS stage) (0.61 % (0.41 – 0.8 5%); p-value$_{tp\text{-}eas}$=0.323) (Fig. 4D; Fig. 3A; Tables 1, S3), but shows gradual significant increase during its further development: 2.14 % (1.49 – 2.95 %) in IAS primmorphs (Fig. 3A; Table 1) (p-value$_{eas\text{-}ias}$=1.02×10^{-4}; Table S3), 6.87 % (5.55 – 8.43 %) in LAS primmorphs (Fig. 3A; Table 1) (p-value$_{ias\text{-}las}$=1.73×10^{-8}; Table S3). In LAS primmorphs, the number of EdU+ cells already reaches level characteristic of intact tissues (p-value$_{las\text{-}it}$=0.052; Table S3) and does not significantly grow during final stages of primmorph development: OTR primmorphs contain 7.75 % (6.71 – 9.03 %) EdU+ cells (p-value$_{las\text{-}otr}$=0.951) and RSs contain 8.82 % (7.62 – 10.14 %) EdU+ cells (p-value$_{otr\text{-}rs}$=0.808) (Fig. 3A; Tables 1, S3).

The distribution of proliferative cells also changes during the development of aquiferous system. Starting with IAS primmorphs, most proliferative cells are located in the rudiments of choanocyte chambers (Fig. 4E). During later developmental stages (LAS, OTR, RS), proliferative cells are mostly located in choanocyte chambers (Fig. 4F-H). Thus, the spatial pattern of cell proliferation after the intermediate stages of reaggregation (*i.e.*, when choanocyte chambers emerge) restores to the state characteristic of *H. dujardinii* intact tissues (Fig. 1C).

The low number of mitotic cells at all stages hinders the analysis. Yet observed changes in the number and distribution of pH+ cells seem to generally follow the ones described for EdU+ cells (Figs. 3, 4). The number of mitotic (pH3+) cells during *H. dujardinii* cell reaggregation shows some variations (Table 1), but the majority of these changes are not significant (except for a few pairs of stages which seem to be due to mere chance). The minimum in the number of pH3+ cells

occurs at the middle stages of cell reaggregation, similarly to the dynamic of EdU+ cells. However, the minimum in pH3+ cells is shifted to EAS and IAS stages: 0.03 % (0.01 – 0.06 %) and 0.05 % (0 – 0.13 %) pH3+ cells, respectively (Fig. 3B; Table S3). pH3+ cells show more or less even distribution at the early stages of cell reaggregation but tend to be located in the rudiments of choanocyte chambers after their formation (Fig. 4).

Overall, the process of cell reaggregation in *H. dujardinii* is accompanied by significant changes in the number and distribution of proliferative cells: the cell proliferation rapidly decreases during early stages (reaching its minimum in TPs and ESP primmorphs) and gradually increases during the restoration of intact sponge structure. The pattern of cell proliferation characteristic of intact sponge tissues (both in terms of number and distribution) is restored as early as the LAS stage.

Cell death is involved in the early stages of cell reaggregation

Intact tissues of *H. dujardinii* contain few TUNEL+ objects: 2.28 (0.89 – 4.07) objects per 1000 cells (Fig. 5; Table 1). The TUNEL+ objects are distributed more or less uniformly in sponge tissues and could be found both in mesohyl and choanocyte chambers (Figs. 1D, S1). Only a few TUNEL+ nuclei are found, while the majority of TUNEL+ objects are smaller and most likely represent apoptotic bodies (Fig. 1D).

The early stages of cell reaggregation in *H. dujardinii* (PMAs/ESPs) are characterized by noticeable upregulation of cell death: the number of TUNEL+ objects in these aggregates is 4.97 (2.88 – 7.44) per 1000 cells (Figs. 5, 6A; Table 1). Similarly to intact tissues, the majority of TUNEL+ objects are apoptotic bodies especially abundant near the surface of aggregates. While the increase in number of TUNEL+ objects in PMAs/ESPs is not significant in comparison with intact tissues ($p\text{-value}_{it\text{-}pma/esp}=0.35$; Table S3), it is significant in comparison with all later stages of cell reaggregation ($p\text{-value}_{pma/esp\text{-}tp}=0.007$; $p\text{-value}_{pma/esp\text{-}eas}=0.001$; $p\text{-value}_{pma/esp\text{-}ias}=0.002$; $p\text{-value}_{pma/esp\text{-}las}=0.0006$; $p\text{-value}_{pma/esp\text{-}otr}=0.0006$; $p\text{-value}_{pma/esp\text{-}rs}=0.0006$) (Fig. 5; Table S3).

Aggregates of TP to RS stages show rather low levels of cell death and contain 0.06-0.95 TUNEL+ objects per 1000 cells (Figs. 5, 6B; Table 1). These variations are not significant between stages and intact sponge tissues, as well as between each pair of stages (Table S3). However, it seems that starting from the EAS stage, primmorphs tend to have a lower level of cell death in comparison with intact tissues (Fig. 5; Table 1).

DISCUSSION

Cell proliferation plays an essential role in various regenerative processes. Proliferation of somatic stem cells generates new cellular material during the physiological regeneration of intact

tissues across all metazoans, from early-branching sponges (Martinand-Mari *et al.*, 2012; Le Goff *et al.*, 2022; Melnikov *et al.*, 2022; Melnikov and Lavrov, 2024b) and cnidarians (Bosch *et al.*, 2009; Fujita *et al.*, 2019; Buzgariu *et al.*, 2022) to insects (Corley and Lavine, 2006; Ohlstein and Spradling, 2006; Sahai-Hernandez *et al.*, 2012) and vertebrates (Pellettieri and Sánchez Alvarado, 2007; Clevers *et al.*, 2014).

Despite the universal role of cell proliferation in the maintenance of tissue homeostasis, its significance in reparative regeneration may vary depending on an organism and regeneration context. In the majority of studied animals, reparative regeneration relies on cell proliferation producing a mass of undifferentiated cells (blastema) for the restoration of lost structures. The cases of proliferation-independent ("morphallactic") regeneration, relying solely on cell plasticity are much rarer. There is no clear correlation with animal phylogenetic position or type of injury: the regeneration of oral structures requires proliferation in *Nematostella vectensis* (Passamaneck and Martindale, 2012) and *Hydractinia* sp. (Gahan *et al.*, 2016) but is proliferation-independent in *Hydra* sp. (Bode, 2003; Galliot, 2013b); in crinoids (Echinodermata), amputated arm regenerates through cell proliferation and blastema formation (Carnevali, 2006; Carnevali and Burighel, 2010), while in the visceral mass regeneration after autotomy, proliferation plays only a minor role (Kalacheva *et al.*, 2017); in contrast, all types of regeneration necessarily involve neoblasts (pluripotent somatic stem cells) proliferation in planarians (Cebrià *et al.*, 2018; Rink, 2018; Ivankovic *et al.*, 2019). Moreover, the nature of the proliferating cell population is also a subject of variation and can be drastically different even in closely related species (Sandoval-Guzmán *et al.*, 2014).

Since the whole-body regeneration (WBR) implies the restoration of the animal body from its small portion or even suspension of single cells and the fact that all structures have to be restored from a very limited amount of cell material, proliferation seems to be indispensable for successful WBR. Indeed, cell proliferation contributes to WBR in ctenophores (Ramon-Mateu *et al.*, 2019; Edgar *et al.*, 2021), planarians (Ivankovic *et al.*, 2019), and ascidians (Blanchoud *et al.*, 2018).

Similar to other cases of WBR, cell reaggregation in *Halisarca dujardinii* is also accompanied by cell proliferation which shows a complex dynamic. The low number of pH3+ (mitotic) cells in intact sponge tissues and at all stages of the reaggregation process shade changes in proliferative activity during *H. dujardinii* cell reaggregation, but they are obvious for EdU+ (DNA-synthesizing) cells. The whole process could be subdivided into three periods according to proliferative activity:

- the early period (PMA stage) is characterized by high proliferative activity quantitively similar to that in intact tissues. However, the spatial distribution of cycling cells is drastically different as they show diffusive distribution in PMAs. Most likely cell proliferation in PMAs is

not a part of the developmental program of the aggregates but represents the residual proliferation of intact tissues: cells that have entered the cell cycle just before the dissociation have to finish this process despite drastic changes in tissue integrity due to dissociation.

- the middle period (ESP, TP, and EAS stages) is characterized by the gradual attenuation of the residual proliferation and the beginning of the aggregate-intrinsic cell proliferation. The ESPs show a significant decrease in the residual proliferation which completely ceases in TPs. The TP stage is characterized by the formation of the complete exopinacoderm isolating the internal milieu of an aggregate from the external environment. From this stage on, an aggregate has the ability to elaborate the internal signaling system that was violated during the dissociation process. The intrinsic signaling system now can coordinate cell behavior and tissue functioning. Regarding cell proliferation, this system can possibly suppress the residual proliferation and then orchestrate the aggregate-intrinsic proliferation.

- the late period (IAS-RS stages) is characterized by the gradual increase in the aggregate-intrinsic cell proliferation and restoration of proliferation pattern characteristic of intact tissues. Already in the beginning of the late period (IAS stage), the switch to aggregate-intrinsic cell proliferation is obvious as – instead of being diffusively distributed – cycling cells are preferentially located in the rudiments of choanocyte chambers. By the LAS stage, the number of proliferating cells in developing aggregates reaches the level of intact tissues, thus completely restoring the regular pattern of cell proliferation in *H. dujardinii*.

One possibility is that the aggregate-intrinsic proliferation could contribute to the developmental process, first of all to the growth of choanocyte chambers. The participation of cell proliferation in the formation of choanocyte chambers is described in freshwater demosponges during development from gemmules (Rozenfeld and Rasmont, 1977) and cell reaggregation (Müller, 1911; Efremova, 1970, 1972). In the case of *Ephydatia fluviatilis* primmorphs, the contribution of cell proliferation to the choanocyte chamber formation was deduced on the basis of direct observations of mitosis in developing chambers, and this period of primmorph development was marked by increased proliferative activity in comparison with intact tissues (Efremova, 1970, 1972). However, the development of the aquiferous system in *H. dujardinii* primmorphs is associated with the gradual recovery of the intact level of cell proliferation, not with increased proliferative activity.

It is more likely that the gradual increase of cell proliferation in *H. dujardinii* developing primmorphs does not itself contribute to the developmental process but instead marks the reconstruction of intact tissues with normal proliferative activity involved in tissue turnover and homeostasis. Such a situation is well-known for reparative regeneration in sponges. In Demospongiae and Calcarea, cell proliferation drastically decreases or is completely absent in the

wound area; subsequent reconstitution of intact tissue structure in the wound area is accompanied by returning of cell proliferation to its basic level and pattern (Alexander *et al.*, 2015; Borisenko *et al.*, 2015; Lavrov *et al.*, 2018; Ereskovsky *et al.*, 2020; Caglar *et al.*, 2021). In all these cases, cell proliferation in the wound area is not a driver for regeneration but more a consequence of it. Anyway, functional experiments involving cell cycle inhibitors are required to univocally elucidate the contribution of cell proliferation to various restorative processes in sponges.

Programmed cell death (studied mainly in the form of apoptosis) is also an important mechanism of morphogenesis in various developmental processes. The main contribution of apoptosis to developmental processes is the elimination of damaged or unnecessary cells (so-called destructive function), *e.g.*, removal of excess mesodermal tissues during tetrapod limb development or resorbing of the tail during tadpole metamorphosis in anurans (Duffy, 2012; Montero *et al.*, 2020; Krasovec *et al.*, 2022). However, recent findings suggest that apoptosis also has an instructive function: apoptotic cells can produce various signals guiding subsequent morphogenetic events and promote cell migration, proliferation, differentiation, and survival (Fan and Bergmann, 2008; Galliot, 2013a; Krasovec *et al.*, 2022).

Both destructive and instructive functions of apoptosis are manifested in regeneration. First of all, several waves of apoptosis could occur after an injury, *e.g.*, in various scenarios of planarian regeneration or in caudal fin regeneration in teleosts (Vriz *et al.*, 2014). In both models, the first wave of apoptosis occurring shortly after wounding is local to the wound area and likely demonstrates the destructive function as being involved in the elimination of damaged cells in the wound vicinity (Pellettieri *et al.*, 2010; Gauron *et al.*, 2013). By contrast, the second apoptotic wave has the instructive function and is necessary for successful regeneration. In zebrafish, this wave is required for normal blastema formation and induction of proliferation in the wound area (Gauron *et al.*, 2013). In planarians, the second wave of apoptosis occurs in a non-localized diffusive manner occurring all over the body of a regenerating animal. The main function of this event is the restoration of proper anatomical scale and proportion through active remodeling of existing tissues (Pellettieri *et al.*, 2010). In other cases, a regenerative system shows only a single apoptotic wave that still can have the instructive function. For instance, during the regeneration of the oral structures in *Hydra* after bisection, a single early wave of cell death induces local compensatory proliferation and Wnt signaling required for proper oral patterning (Chera *et al.*, 2009; Cazet *et al.*, 2021).

Cell reaggregation and primmorph development in *H. dujardinii* are associated with a single wave of cell death occurring during the transformation of PMAs into TPs. Such a pattern of cell death could indicate that this transformation is associated with the elimination of damaged and/or unnecessary cells as was assumed earlier for many sponge species based on *in vivo*, histological,

ultrastructural, and RNA-seq data (Sipkema *et al.*, 2003; Eerkes-Medrano *et al.*, 2015; Lavrov and Kosevich, 2016; Soubigou *et al.*, 2020).

After the primmorph formation and during their progressive development, the level of cell death substantially decreases, becoming even lower than in intact tissues (though the change is not significant). Possibly, cell death is suppressed in developing primmorphs to retain as many cells as possible for subsequent sponge reconstruction. The data about the involvement of cell death in the restorative process in sponges are very limited. However, it seems that cell death suppression could be a common theme for later stages of sponge regeneration, as the downregulation of apoptotic pathway genes is shown to occur after the debris removal and/or wound epithelization during WBR from small body fragments in demosponge *Halichondria panicea* (Riesgo *et al.*, 2022) and calcareous sponge *Sycon ciliatum* (Caglar *et al.*, 2021).

CONCLUSION

The current study has broadened the knowledge of cellular mechanisms involved in WBR in sponges. Despite the complex dynamic of both cell proliferation and cell death during reaggregation in demosponge *Halisarca dujardinii*, they likely contribute a little to aggregate formation and progressive development. Relatively high proliferative activity in the early and late periods of the reaggregation process seems to be more a consequence of the normal turnover of intact sponge tissues rather than a developmental mechanism. During the early period, proliferation in aggregates represents the residual proliferation of intact tissues; during the late period, aggregate-intrinsic proliferation most likely reflects the reconstruction of sponge intact tissues with their normal turnover. The contribution of cell death to aggregate development is limited to a short period of elimination of damaged and/or unnecessary cells during the formation of epithelized aggregates. Active cell migration, dedifferentiation, and transdifferentiation seem to be key morphogenetic mechanisms during cell reaggregation in sponges, rendering this restorative process mainly as morphallactic remodeling of cellular aggregates.

ACKNOWLEDGMENTS

The authors acknowledge the support of Lomonosov Moscow State University Program of Development (Nikon A1 and Olympus Fluoview FV10 CLSMs), Centre of Microscopy WSBS MSU, Morphology Service of IMBE, Marseille, and IMM, Marseille. The authors sincerely thank Darya Potashnikova, Ilya Borisenko, Vitaly Kozin, Alexandra Shalaeva, Victor Starunov, and Roman Kostyuchenko for fruitful discussions and helpful tips. This study was conducted within the frame of the IDB RAS Government Basic Research Program no. 0088-2024-0012.

FUNDING INFORMATION

The research was supported by the Russian Science Foundation, grant no. 23-74-10005.

CONFLICT OF INTEREST STATEMENT

The authors declare no potential conflicts of interest.

DATA AVAILABILITY STATEMENT

Confocal Z-stacks, the results of cell counting and the R script used in statistical analysis supporting the conclusions of this article are available in the Mendeley Data repository under the following links: *(links will be supplemented after the first revision round)*.

REFERENCES

Alexander BE, Achlatis M, Osinga R, van der Geest HG, Cleutjens JPM, Schutte B, de Goeij JM (2015) Cell kinetics during regeneration in the sponge Halisarca caerulea : how local is the response to tissue damage? PeerJ 3:e820 https://doi.org/10.7717/peerj.820

Blanchoud S, Rinkevich B, Wilson MJ (2018) Whole-Body Regeneration in the Colonial Tunicate Botrylloides leachii. Springer International Publishing, pp 337-355 https://doi.org/10.1007/978-3-319-92486-1_16

Bode HR (2003) Head regeneration in Hydra. Developmental Dynamics 226:225-236 https://doi.org/10.1002/dvdy.10225

Borisenko I, Bolshakov FV, Ereskovsky AV, Lavrov AI (2021) Expression of Wnt and TGF-Beta Pathway Components during Whole-Body Regeneration from Cell Aggregates in Demosponge Halisarca dujardinii. Genes 12:944 https://doi.org/10.3390/genes12060944

Borisenko I, Daugavet M, Ereskovsky A, Lavrov A, Podgornaya O (2022) Novel protein from larval sponge cells, ilborin, is related to energy turnover and calcium binding and is conserved among marine invertebrates. Open Biology 12:210336 https://doi.org/10.1098/rsob.210336

Borisenko IE, Adamska M, Tokina DB, Ereskovsky AV (2015) Transdifferentiation is a driving force of regeneration in Halisarca dujardini (Demospongiae, Porifera). PeerJ 3:e1211 https://doi.org/10.7717/peerj.1211

Bosch TCG, Anton-Erxleben F, Hemmrich G, Khalturin K (2009) The Hydra polyp: Nothing but an active stem cell community. Development, Growth & Differentiation 52:15-25 https://doi.org/10.1111/j.1440-169X.2009.01143.x

Brown FD, Keeling EL, Le AD, Swalla BJ (2009) Whole body regeneration in a colonial ascidian, Botrylloides violaceus. Journal of Experimental Zoology Part B: Molecular and Developmental Evolution 312B:885-900 https://doi.org/10.1002/jez.b.21303

Buzgariu W, Aubry-Lachainaye JP, Galliot B (2022) Studying Stem Cell Biology in Intact and Whole-Body Regenerating Hydra by Flow Cytometry. Methods Mol Biol 2450:373-398 https://doi.org/10.1007/978-1-0716-2172-1_20

Caglar C, Ereskovsky AV, Laplante M, Tokina D, Leininger S, Borisenko IE, Aisbett GA, Pan D, Adamski M, Adamska M (2021) Fast transcriptional activation of developmental signalling pathways during wound healing of the calcareous sponge Sycon ciliatum. bioRxiv

Canty A, Ripley B (2021) boot: Bootstrap R (S-Plus) Functions. R package version 1.3-28.

Carnevali MDC (2006) Regeneration in Echinoderms: repair, regrowth, cloning. Invertebrate Survival Journal 3:64-76

Carnevali MDC, Burighel P (2010) Regeneration in Echinoderms and Ascidians. Encyclopedia of Life Sciences. John Wiley & Sons, Ltd, Chichester, UKhttps://doi.org/10.1002/9780470015902.a0022102

Carnevali MDC, Sugni M, Bonasoro F (2024) Regeneration Potential in Echinoderms: Revisiting the Regeneration Concept. In: Saleuddin S, Leys SP, Roer RD, Wilkie IC (eds) Frontiers in Invertebrate Physiology: A Collection of Reviews, vol 3. Apple Academic Press, New York, pp 185-302

Cary GA, Wolff A, Zueva OR, Pattinato J, Hinman VF (2019) Analysis of sea star larval regeneration reveals conserved processes of whole-body regeneration across the metazoa. BMC Biology 17:16 https://doi.org/10.1186/s12915-019-0633-9

Cazet JF, Cho A, Juliano CE (2021) Generic injuries are sufficient to induce ectopic Wnt organizers in Hydra. eLife 10:e60562 https://doi.org/10.7554/eLife.60562

Cebrià F, Adell T, Saló E (2018) Rebuilding a planarian: from early signaling to final shape. The International Journal of Developmental Biology 62:537-550 https://doi.org/10.1387/ijdb.180042es

Chera S, Ghila L, Dobretz K, Wenger Y, Bauer C, Buzgariu W, Martinou J-C, Galliot B (2009)

Apoptotic Cells Provide an Unexpected Source of Wnt3 Signaling to Drive Hydra Head Regeneration. Developmental Cell 17:279-289 https://doi.org/10.1016/j.devcel.2009.07.014

Clevers H, Loh KM, Nusse R (2014) An integral program for tissue renewal and regeneration: Wnt signaling and stem cell control. Science 346:1248012 https://doi.org/10.1126/science.1248012

Corley LS, Lavine MD (2006) A review of insect stem cell types. Seminars in Cell & Developmental Biology 17:510-517 https://doi.org/https://doi.org/10.1016/j.semcdb.2006.07.002

Davison AC, Hinkley DV (1997) Bootstrap Methods and Their Applications. Cambridge University Press, Cambridge. ISBN 0-521-57391-2

Duffy DJ (2012) Instructive reconstruction: A new role for apoptosis in pattern formation. BioEssays 34:561-564 https://doi.org/10.1002/bies.201200018

Edgar A, Mitchell DG, Martindale MQ (2021) Whole-Body Regeneration in the Lobate Ctenophore Mnemiopsis leidyi. Genes 12:867 https://doi.org/10.3390/genes12060867

Eerkes-Medrano DI, Feehan CJ, Leys SP (2015) Sponge cell aggregation: checkpoints in development indicate a high level of organismal complexity. Invertebrate Biology 134:1-18 https://doi.org/10.1111/ivb.12072

Efremova SM (1970) Proliferation Activity and Synthesis of Protein in the Cells of Fresh-Water Sponges during Development after Dissociation. In: Fry WG (ed) The biology of the Porifera. Academic Press Inc, London, pp 399-413

Efremova SM (1972) Morphophysiological analysis of the development of freshwater sponges Ephydatia fluviatilis and Spongilla lacustris from dissociated cells. Transactions of Leningrad Society of Naturalists 78:110-154

Ereskovsky AV, Borisenko IE, Bolshakov FV, Lavrov AI (2021) Whole-Body Regeneration in Sponges: Diversity, Fine Mechanisms, and Future Prospects. Genes 12:506 https://doi.org/10.3390/genes12040506

Ereskovsky AV, Borisenko IE, Lapébie P, Gazave E, Tokina DB, Borchiellini C (2015) Oscarella lobularis (Homoscleromorpha, Porifera) Regeneration: Epithelial Morphogenesis and Metaplasia. Plos One 10:e0134566 https://doi.org/10.1371/journal.pone.0134566

Ereskovsky AV, Chernogor LI, Belikov SI (2016) Ultrastructural description of development and cell composition of primmorphs in the endemic Baikal sponge Lubomirskia baicalensis. Zoomorphology 135:1-17 https://doi.org/10.1007/s00435-015-0289-0

Ereskovsky AV, Lavrov AI (2021) Porifera. In: LaDouceur EB (ed) Invertebrate Histology. Wiley, pp 19-54 https://doi.org/10.1002/9781119507697.ch2

Ereskovsky AV, Tokina DB, Saidov DM, Baghdiguian S, Le Goff E, Lavrov AI (2020) Transdifferentiation and mesenchymal-to-epithelial transition during regeneration in Demospongiae (Porifera). Journal of Experimental Zoology Part B: Molecular and Developmental Evolution 334:37-58 https://doi.org/10.1002/jez.b.22919

Fan Y, Bergmann A (2008) Apoptosis-induced compensatory proliferation. The Cell is dead. Long live the Cell! Trends in Cell Biology 18:467-473 https://doi.org/10.1016/j.tcb.2008.08.001

Fujita S, Kuranaga E, Nakajima Y-I (2019) Cell proliferation controls body size growth, tentacle morphogenesis, and regeneration in hydrozoan jellyfish Cladonema pacificum. PeerJ 7:e7579 https://doi.org/10.7717/peerj.7579

Gahan JM, Bradshaw B, Flici H, Frank U (2016) The interstitial stem cells in Hydractinia and their role in regeneration. Current Opinion in Genetics & Development 40:65-73 https://doi.org/10.1016/j.gde.2016.06.006

Galliot B (2013a) Injury-induced asymmetric cell death as a driving force for head regeneration in Hydra. Development Genes and Evolution 223:39-52 https://doi.org/10.1007/s00427-012-0411-y

Galliot B (2013b) Regeneration in Hydra. eLS. John Wiley & Sons, Ltdhttps://doi.org/https://doi.org/10.1002/9780470015902.a0001096.pub3

Gauron C, Rampon C, Bouzaffour M, Ipendey E, Teillon J, Volovitch M, Vriz S (2013) Sustained production of ROS triggers compensatory proliferation and is required for regeneration to proceed. Scientific Reports 3:https://doi.org/10.1038/srep02084

Ivankovic M, Haneckova R, Thommen A, Grohme MA, Vila-Farré M, Werner S, Rink JC (2019) Model systems for regeneration: planarians. Development 146:dev167684 https://doi.org/10.1242/dev.167684

Kalacheva NV, Eliseikina MG, Frolova LT, Dolmatov IY (2017) Regeneration of the digestive system in the crinoid Himerometra robustipinna occurs by transdifferentiation of neurosecretory-like cells. PLOS ONE 12:e0182001 https://doi.org/10.1371/journal.pone.0182001

Kassambara A (2023) rstatix: Pipe-Friendly Framework for Basic Statistical Tests. R package version 0.7.2 https://CRAN.R-project.org/package=rstatix

Kirillova A, Genikhovich G, Pukhlyakova E, Demilly A, Kraus YA, Technau U (2018) Germ-layer commitment and axis formation in sea anemone embryonic cell aggregates. Proceedings of the National Academy of Sciences 115:1813-1818 https://doi.org/10.1073/pnas.1711516115

Kolbasova GD, Tzetlin AB, Kupriyanova EK (2014) Chaetal loss and replacement in Pseudopotamilla reniformis (Sabellida, Annelida). Invertebrate Biology 133:261-273

https://doi.org/https://doi.org/10.1111/ivb.12061

Kostyuchenko RP, Kozin VV (2021) Comparative Aspects of Annelid Regeneration: Towards Understanding the Mechanisms of Regeneration. Genes 12:1148 https://doi.org/10.3390/genes12081148

Krasovec G, Horkan HR, Queinnec E, Chambon JP (2022) The constructive function of apoptosis: More than a dead-end job. Front Cell Dev Biol 10:1033645 https://doi.org/10.3389/fcell.2022.1033645

Kuznetsov AV, Vainer VI, Volkova YM, Tsygankova VM, Bochko DN, Mukhanov VS (2022) Trichoplax sp. H2 cultivation and regeneration from body fragments and dissociated cell aggregates: outlook for genetic modification. Marine Biological Journal 7:60-79 https://doi.org/10.21072/mbj.2022.07.3.06

Lavrov AI, Bolshakov FV, Tokina DB, Ereskovsky AV (2018) Sewing up the wounds: The epithelial morphogenesis as a central mechanism of calcaronean sponge regeneration. Journal of Experimental Zoology Part B: Molecular and Developmental Evolution 330:351-371 https://doi.org/10.1002/jez.b.22830

Lavrov AI, Bolshakov FV, Tokina DB, Ereskovsky AV (2022) Fine details of the choanocyte filter apparatus in asconoid calcareous sponges (Porifera: Calcarea) revealed by ruthenium red fixation. Zoology 150:125984 https://doi.org/https://doi.org/10.1016/j.zool.2021.125984

Lavrov AI, Ereskovsky AV (2022) Studying Porifera WBR Using the Calcerous Sponges Leucosolenia. Whole-Body Regeneration Springer US, pp 69-93 https://doi.org/10.1007/978-1-0716-2172-1_4

Lavrov AI, Kosevich IA (2014) Sponge cell reaggregation: Mechanisms and dynamics of the process. Russian Journal of Developmental Biology 45:205-223 https://doi.org/10.1134/S1062360414040067

Lavrov AI, Kosevich IA (2016) Sponge cell reaggregation: Cellular structure and morphogenetic potencies of multicellular aggregates. Journal of Experimental Zoology Part A: Ecological Genetics and Physiology 325:158-177 https://doi.org/10.1002/jez.2006

Lavrov AI, Saidov DM, Bolshakov FV, Kosevich IA (2020) Intraspecific variability of cell reaggregation during reproduction cycle in sponges. Zoology 140:125795 https://doi.org/10.1016/j.zool.2020.125795

Le Goff E, Martinand-Mari C, Belkhir K, Vacelet J, Nidelet S, Godefroy N, Baghdiguian S (2022) Molecular complexity and gene expression controlling cell turnover during a digestive cycle of carnivorous sponge Lycopodina hypogea. Cell and Tissue Research https://doi.org/10.1007/s00441-022-03610-3

Martinand-Mari C, Vacelet J, Nickel M, Worheide G, Mangeat P, Baghdiguian S (2012) Cell death

and renewal during prey capture and digestion in the carnivorous sponge Asbestopluma hypogea (Porifera: Poecilosclerida). Journal of Experimental Biology 215:3937-3943 https://doi.org/10.1242/jeb.072371

Melnikov NP, Bolshakov FV, Frolova VS, Skorentseva KV, Ereskovsky AV, Saidova AA, Lavrov AI (2022) Tissue homeostasis in sponges: Quantitative analysis of cell proliferation and apoptosis. J Exp Zool B Mol Dev Evol 338:360-381 https://doi.org/10.1002/jez.b.23138

Melnikov N, Lavrov A (2024a) An experimental approach in analyzing the cell cycle dynamics of food-entrapping cells of sponges: Halisarca", Mendeley Data, V2, https://doi.org/10.17632/7fbv46wsnv.2

Melnikov NP, Lavrov AI (2024)b Cell cycle dynamics of food-entrapping cells of sponges: an experimental approach. The FEBS Journal https://doi.org/10.1111/febs.17098

Mitoh S, Yusa Y (2021) Extreme autotomy and whole-body regeneration in photosynthetic sea slugs. Curr Biol 31:R233-R234 https://doi.org/10.1016/j.cub.2021.01.014

Montero JA, Lorda-Diez CI, Sanchez-Fernandez C, Hurle JM (2020) Cell death in the developing vertebrate limb: A locally regulated mechanism contributing to musculoskeletal tissue morphogenesis and differentiation. Developmental Dynamics dvdy.237 https://doi.org/10.1002/dvdy.237

Müller K (1911) Das Regenerationsvermögen der Süßwasserschwämme, insbesondere Untersuchungen über die bei ihnen vorkommende Regeneration nach Dissociation und Reunition. Archiv für Entwicklungsmechanik 32:398-446

Ohlstein B, Spradling A (2006) The adult Drosophila posterior midgut is maintained by pluripotent stem cells. Nature 439:470-474 https://doi.org/10.1038/nature04333

Osigus H-J, Eitel M, Horn K, Kamm K, Kosubek-Langer J, Schmidt MJ, Hadrys H, Schierwater B (2022) Studying Placozoa WBR in the Simplest Metazoan Animal, Trichoplax adhaerens. Springer US, pp 121-133 https://doi.org/10.1007/978-1-0716-2172-1_6

Passamaneck YJ, Martindale MQ (2012) Cell proliferation is necessary for the regeneration of oral structures in the anthozoan cnidarian Nematostella vectensis. BMC Developmental Biology 12:34 https://doi.org/10.1186/1471-213X-12-34

Pellettieri J, Fitzgerald P, Watanabe S, Mancuso J, Green DR, Sánchez Alvarado A (2010) Cell death and tissue remodeling in planarian regeneration. Developmental Biology 338:76-85 https://doi.org/10.1016/j.ydbio.2009.09.015

Pellettieri J, Sánchez Alvarado A (2007) Cell Turnover and Adult Tissue Homeostasis: From Humans to Planarians. Annual Review of Genetics 41:83-105 https://doi.org/10.1146/annurev.genet.41.110306.130244

Ramon-Mateu J, Ellison ST, Angelini TE, Martindale MQ (2019) Regeneration in the ctenophore

Mnemiopsis leidyi occurs in the absence of a blastema, requires cell division, and is temporally separable from wound healing. BMC Biology 17:80 https://doi.org/10.1186/s12915-019-0695-8

R Core Team (2022) R: A language and environment for statistical computing. R Foundation for Statistical Computing, Vienna, Austria. https://www.R-project.org/.

Riesgo A, Santodomingo N, Koutsouveli V, Kumala L, Leger MM, Leys SP, Funch P (2022) Molecular machineries of ciliogenesis, cell survival, and vasculogenesis are differentially expressed during regeneration in explants of the demosponge Halichondria panicea. BMC Genomics 23:858 https://doi.org/10.1186/s12864-022-09035-0

Rink JC (2018) Stem Cells, Patterning and Regeneration in Planarians: Self-Organization at the Organismal Scale. In: Rink JC (ed) Planarian Regeneration: Methods and Protocols. Methods in Molecular Biology, vol 1774. Springer New York, New York, NY, pp 18-22 https://doi.org/10.1007/978-1-4939-7802-1

Rozenfeld F, Rasmont R (1977) Hydroxyurea: An Inhibitor of the Differentiation of Choanocytes in Fresh-Water Sponges and a Possible Agent for the Isolation of Embryonic Cells. Differentiation 7:53-60 https://doi.org/10.1111/j.1432-0436.1977.tb01496.x

Sahai-Hernandez P, Castanieto A, Nystul TG (2012) Drosophila models of epithelial stem cells and their niches. WIREs Developmental Biology 1:447-457 https://doi.org/10.1002/wdev.36

Sandoval-Guzmán T, Wang H, Khattak S, Schuez M, Roensch K, Nacu E, Tazaki A, Joven A, Tanaka EM, Simon A (2014) Fundamental differences in dedifferentiation and stem cell recruitment during skeletal muscle regeneration in two salamander species. Cell Stem Cell 14:174-187 https://doi.org/10.1016/j.stem.2013.11.007

Seybold A, Salvenmoser W, Hobmayer B (2016) Sequential development of apical-basal and planar polarities in aggregating epitheliomuscular cells of Hydra. Developmental Biology 412:148-159 https://doi.org/10.1016/j.ydbio.2016.02.022

Sipkema D, van Wielink R, van Lammeren AAM, Tramper J, Osinga R, Wijffels RH (2003) Primmorphs from seven marine sponges: formation and structure. Journal of biotechnology 100:127-139

Skorentseva KV, Bolshakov FV, Saidova AA, Lavrov AI (2023) Regeneration in calcareous sponge relies on 'purse-string' mechanism and the rearrangements of actin cytoskeleton. Cell and Tissue Research 394:107-129 https://doi.org/10.1007/s00441-023-03810-5

Soubigou A, Ross EG, Touhami Y, Chrismas N, Modepalli V (2020) Regeneration in the sponge Sycon ciliatum partly mimics postlarval development. Development 147:dev193714 https://doi.org/10.1242/dev.193714

Srivastava M, Mazza-Curll Kathleen L, van Wolfswinkel Josien C, Reddien Peter W (2014) Whole-Body Acoel Regeneration Is Controlled by Wnt and Bmp-Admp Signaling. Current Biology 24:1107-1113 https://doi.org/https://doi.org/10.1016/j.cub.2014.03.042

Vila-Farré M, Rozanski A, Ivanković M, Cleland J, Brand JN, Thalen F, Grohme MA, Von Kannen S, Grosbusch AL, Vu HTK, Prieto CE, Carbayo F, Egger B, Bleidorn C, Rasko JEJ, Rink JC (2023) Evolutionary dynamics of whole-body regeneration across planarian flatworms. Nature Ecology & Evolution https://doi.org/10.1038/s41559-023-02221-7

Vriz S, Reiter S, Galliot B (2014) Cell Death: A Program to Regenerate. In: Galliot B (ed) Current topics in developmental biology, vol 108. Academic Press Inc, pp 121-151 https://doi.org/10.1016/B978-0-12-391498-9.00002-4

Wickham H (2016) ggplot2: Elegant Graphics for Data Analysis. Springer-Verlag New York.

TABLES

Table 1. Mean proportions of proliferative cells in the S-phase (EdU+), proliferative cells in the G2/M-phase (pH3+) and apoptotic cells (TUNEL+) in intact tissues and on the main stages of cell reaggregation in *Halisarca dujardinii*.

Stage	EdU+ cells, %	pH3+ cells, %	TUNEL+ objects per 1000 cells
IT	9.98 (8.20 – 11.96)	0.22 (0.1 – 0.39)	2.28 (0.89 – 4.07)
PMA	6.45 (4.82 – 8.02)	0.20 (0.13 – 0.28)	4.97 (2.88 – 7.44)
ESP	2.15 (1.26 – 3.12)	0.18 (0.03 – 0.32)	
TP	0.24 (0 – 0.57)	0.10 (0.05 – 0.16)	0.95 (0.32 – 1.72)
EAS	0.61 (0.41 – 0.85)	0.03 (0.01 – 0.06)	0.33 (0.12 – 0.58)
IAS	2.14 (1.49 – 2.95)	0.05 (0 – 0.13)	0.60 (0.14 – 0.99)
LAS	6.87 (5.55 – 8.43)	0.11 (0.07 – 0.15)	0.10 (0 – 0.24)
OTR	7.75 (6.71 – 9.03)	0.24 (0.15 – 0.35)	0.06 (0 – 0.24)
RS	8.82 (7.62 – 10.14)	0.15 (0.08 – 0.24)	0.06 (0 – 0.15)

Values are given as mean ($C.I._{99\%}$ lower and upper limits). IT – intact tissues, PMA – primary multicellular aggregates, ESP – early-staged primmorphs, TP – true primmorphs, EAS – primmorphs with developing aquiferous system, early stages; IAS - primmorphs with developing aquiferous system, intermediate stages; LAS – primmorphs with developing aquiferous system, late stages; OTR – primmorphs with oscular tube rudiments; RS – reconstructed sponges.

FIGURE LEGENDS

Fig. 1. *Halisarca dujardinii*. A – intact sponge *in vivo* on the algal substrate. B – histological structure of intact sponge; white dashed lines outline choanocyte chambers. C – cell proliferation in intact tissues; image is a maximum intensity projection (MIP), obtained from 8 µm Z stack; red arrowheads mark EdU-positive nuclei of DNA-synthesizing cells, yellow arrowheads – pH3-positive nuclei of mitotic cells. D – apoptosis in intact tissues; image is MIP, obtained from 8 µm Z stack; white arrowheads mark TUNEL-positive apoptotic nuclei and smaller apoptotic bodies. alg – algae substrate, cc – choanocyte chambers, cn – canal of aquiferous system, ect – ectosome, end – endosome, ot – oscular tube. Blue – DAPI, 4',6-diamidino-2-phenylindole, green – acetylated α-tubulin, magenta – EdU, 5-ethynyl-2′- deoxyuridine (C), red – TUNEL, terminal deoxynucleotidyl transferase dUTP nick end labeling (D). Scale bar: A – 5 mm, B – 100 µm, C, D – 50 µm.

Fig. 2. The main stages of cell reaggregation and primmorph development in *Halisarca dujardinii*. A, B – primary multicellular aggregates (PMA; 6 hours post-dissociation, hpd). C, D – true

primmorphs (TP; 1 day post-dissociation, dpd). E, F – primmorphs with developing aquiferous system, early stages (EAS; 5 dpd), white arrowheads mark cavities of developing aquiferous system. G, H – primmorphs with developing aquiferous system, late stages (LAS; 11 dpd), white arrowheads mark rudiments of choanocyte chambers. I – primmorphs with oscular tube rudiments, (OTR; 15 dpd), white arrowheads mark choanocyte chambers. J, K – reconstructed sponges (RS; 21 dpd), white arrowheads mark choanocyte chambers. A, C, E, G, I, J – developmental stages *in vivo*, stereomicroscopy; B, D, F, H, K – the histological structure of developmental stages, semi-thin sections, light microscopy. c – cavities of developing aquiferous system, cc – choanocyte chambers, ccr – rudiments of choanocyte chambers, cn – canals of aquiferous system, ot – oscular tubes, otr – rudiments of oscular tubes. Scale bar: A, C, G, I, J – 0.5 mm, E – 1 mm, B, D, F, H, K – 50 μm.

Fig. 3. Quantitative analysis of cell proliferation in intact tissues and at the main stages of cell reaggregation process in *Halisarca dujardinii*. A – S-phase (EdU+) cells (statistical significance is shown only for chosen pairs; for all pairs see Table S3). B – mitotic (pH3+) cells (only significantly different pairs are marked). ns – not significant, asterisk – significant with p-values<0.01. IT – intact tissues, PMA – primary multicellular aggregates, ESP – early-staged primmorphs, TP – true primmorphs, EAS – primmorphs with developing aquiferous system, early stages; IAS – primmorphs with developing aquiferous system, intermediate stages; LAS – primmorphs with developing aquiferous system, late stages; OTR – primmorphs with oscular tube rudiments; RS – reconstructed sponges.

Fig. 4. Cell proliferation during the process of cell reaggregation and sponge reconstruction in *Halisarca dujardinii*. A – primary multicellular aggregate (1 day post-dissociation, dpd). B – early-staged primmorph (2 dpd). C – true primmorph (4 dpd). D – primmorph with developing aquiferous system, early stages (9 dpd). E – primmorph with developing aquiferous system, intermediate stages system (11 dpd). F – primmorph with developing aquiferous system, late stages (11 dpd). G – primmorph with oscular tube rudiments (22 dpd). H – reconstructed sponge (19 dpd). Each image is a maximum intensity projection, obtained from 22 μm (A) or 15 μm (B-H) Z-stack. Red arrowheads marks EdU-positive nuclei of DNA-synthesizing cells, yellow arrowheads – pH3-positive nuclei of mitotic cells. c – cavities of developing aquiferous system, cc – choanocyte chambers, ccr – rudiments of choanocyte chamber. Blue – DAPI, 4',6-diamidino-2-phenylindole, green – acetylated α-tubulin, magenta – EdU, 5-ethynyl-2′-deoxyuridine, yellow – phosphorylated histone3. Scale bar: 50 μm.

Fig. 5. Quantitative analysis of cell death in intact tissues and at the main stages of cell reaggregation process in *Halisarca dujardinii*. Asterisk – significant with p-values<0.01. IT – intact tissues, PMA – primary multicellular aggregates, ESP – early-staged primmorphs, TP – true primmorphs, EAS – primmorphs with developing aquiferous system, early stages; IAS – primmorphs with developing aquiferous system, intermediate stages; LAS – primmorphs with developing aquiferous system, late stages; OTR – primmorphs with oscular tube rudiments; RS – reconstructed sponges.

Fig. 6. Cell death during cell reaggregation in *Halisarca dujardinii*. A – numerous TUNEL+ objects in primary multicellular aggregate/early-staged primmorph (1 day post-dissociation, dpd); image is a maximum intensity projection (MIP), obtained from 25 μm Z-stack. B – single TUNEL+ nucleus in primmorph with developing aquiferous system, early stages (5 dpd) image is a MIP, obtained from 15 μm Z-stack. Blue – DAPI, 4',6-diamidino-2-phenylindole, red – TUNEL, terminal deoxynucleotidyl transferase dUTP nick end labeling. Scale bar: A, B – 50 μm.

SUPPLEMENTARY MATERIAL

Table S1. Number of aggregates at each stage of reaggregation used for proliferation studies.

Table S2. Number of aggregates at each stage of reaggregation used for apoptosis studies.

Table S3. Raw data, descriptive statistics, and statistical test information for cell proliferation and apoptosis in intact sponges and different stages of reaggregation in *H. dujardinii*.

Fig. S1. Colocalization of DAPI and EdU signals (A), DAPI and pH3 signals (B), DAPI and TUNEL signals (C). White arrowheads mark apoptotic bodies. Scale bar: A, B – 5 μm, C – 10 μm.

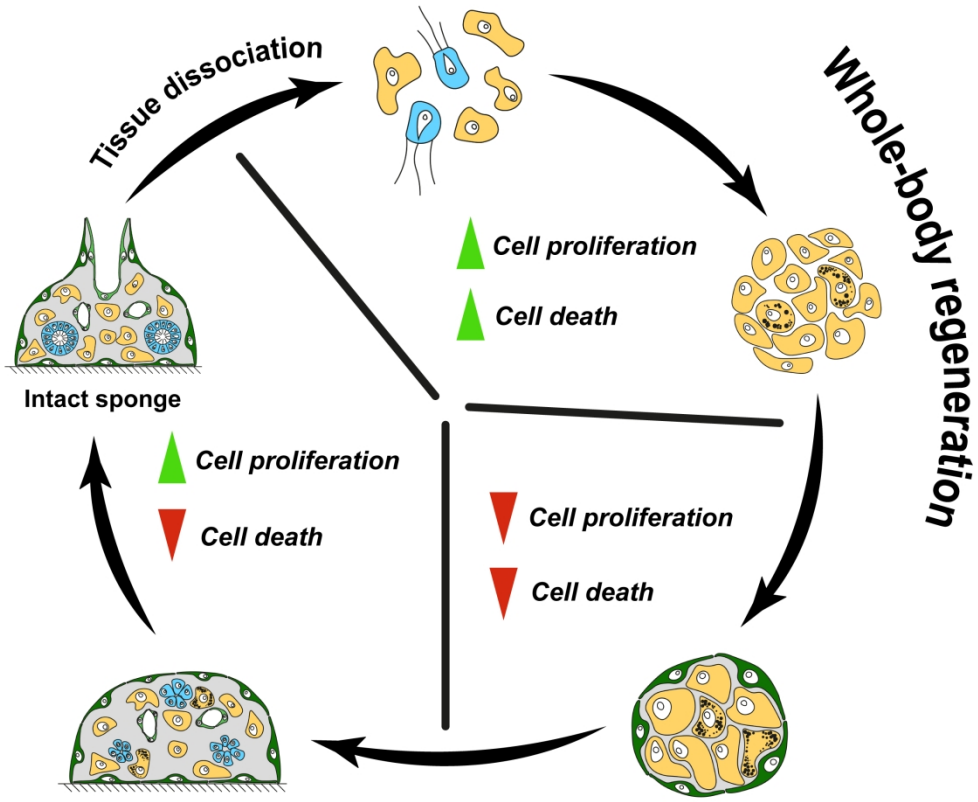

218x179mm (300 x 300 DPI)

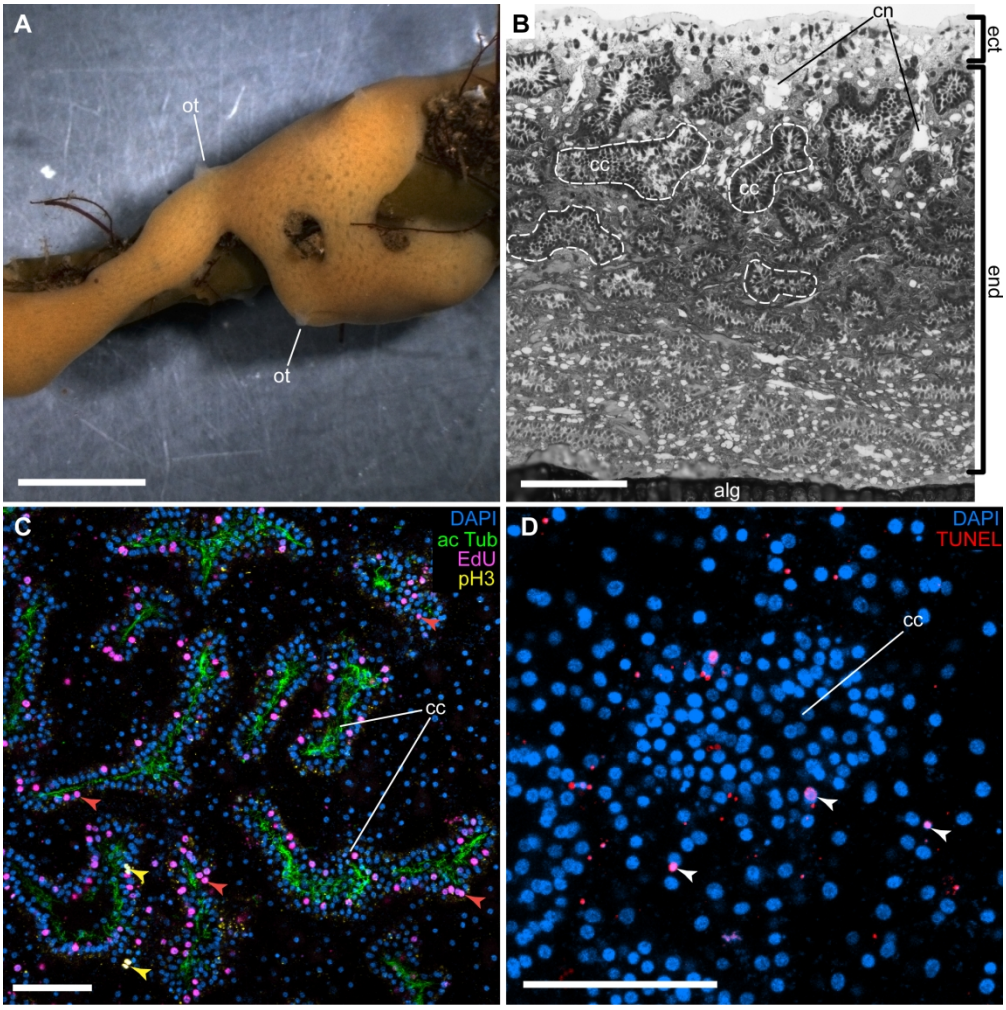

Fig. 1. Halisarca dujardinii. A – intact sponge in vivo on the algal substrate. B – histological structure of intact sponge; white dashed lines outline choanocyte chambers. C – cell proliferation in intact tissues; image is a maximum intensity projection (MIP), obtained from 8 μm Z stack; red arrowheads mark EdU-positive nuclei of DNA-synthesizing cells, yellow arrowheads – pH3-positive nuclei of mitotic cells. D – apoptosis in intact tissues; image is MIP, obtained from 8 μm Z stack; white arrowheads mark TUNEL-positive apoptotic nuclei and smaller apoptotic bodies. alg – algae substrate, cc – choanocyte chambers, cn – canal of aquiferous system, ect – ectosome, end – endosome, ot – oscular tube. Blue – DAPI, 4',6-diamidino-2-phenylindole, green – acetylated α-tubulin, magenta – EdU, 5-ethynyl-2'- deoxyuridine (C), red – TUNEL, terminal deoxynucleotidyl transferase dUTP nick end labeling (D). Scale bar: A – 5 mm, B – 100 μm, C, D – 50 μm.

210x209mm (300 x 300 DPI)

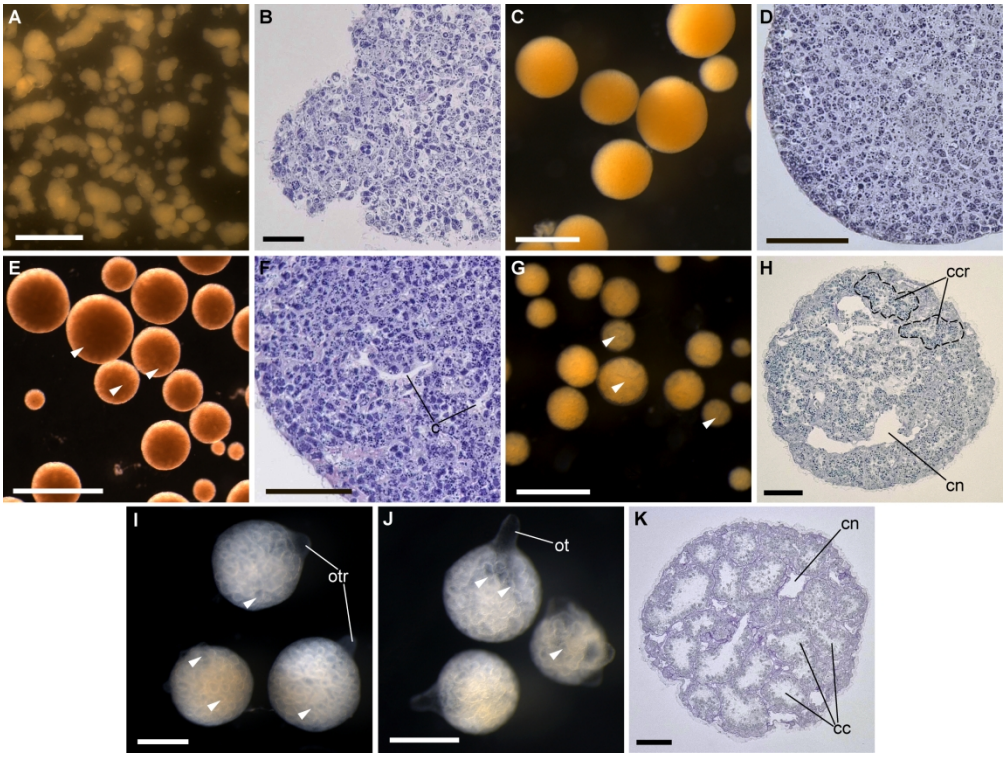

Fig. 2. The main stages of cell reaggregation and primmorph development in Halisarca dujardinii. A, B – primary multicellular aggregates (PMA; 6 hours post-dissociation, hpd). C, D – true primmorphs (TP; 1 day post-dissociation, dpd). E, F – primmorphs with developing aquiferous system, early stages (EAS; 5 dpd), white arrowheads mark cavities of developing aquiferous system. G, H – primmorphs with developing aquiferous system, late stages (LAS; 11 dpd), white arrowheads mark rudiments of choanocyte chambers. I – primmorphs with oscular tube rudiments, (OTR; 15 dpd), white arrowheads mark choanocyte chambers. J, K – reconstructed sponges (RS; 21 dpd), white arrowheads mark choanocyte chambers. A, C, E, G, I, J – developmental stages in vivo, stereomicroscopy; B, D, F, H, K – the histological structure of developmental stages, semi-thin sections, light microscopy. c – cavities of developing aquiferous system, cc – choanocyte chambers, ccr – rudiments of choanocyte chambers, cn – canals of aquiferous system, ot – oscular tubes, otr – rudiments of oscular tubes. Scale bar: A, C, G, I, J – 0.5 mm, E – 1 mm, B, D, F, H, K – 50 μm.

281x210mm (300 x 300 DPI)

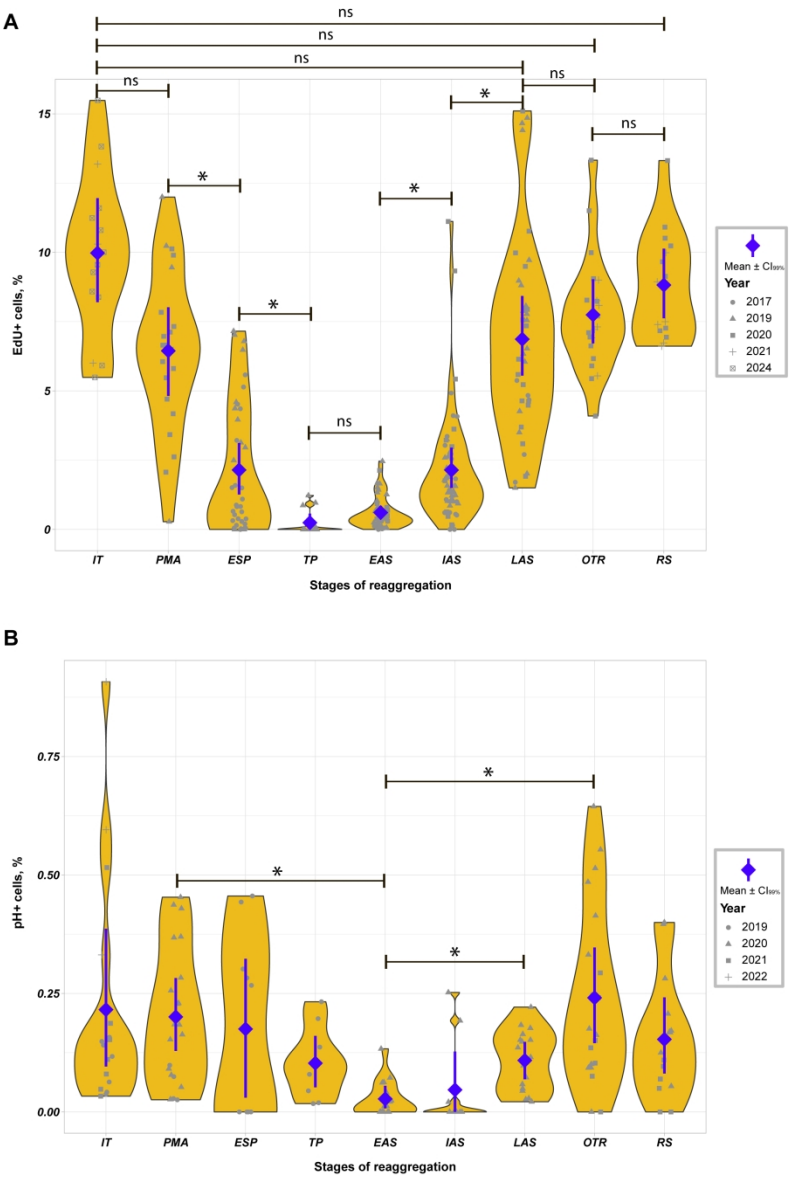

Fig. 3. Quantitative analysis of cell proliferation in intact tissues and at the main stages of cell reaggregation process in Halisarca dujardinii. A – S-phase (EdU+) cells (statistical significance is shown only for chosen pairs; for all pairs see Table S3). B – mitotic (pH3+) cells (only significantly different pairs are marked). ns – not significant, asterisk – significant with p-values<0.01. IT – intact tissues, PMA – primary multicellular aggregates, ESP – early-staged primmorphs, TP – true primmorphs, EAS – primmorphs with developing aquiferous system, early stages; IAS – primmorphs with developing aquiferous system, intermediate stages; LAS – primmorphs with developing aquiferous system, late stages; OTR – primmorphs with oscular tube rudiments; RS – reconstructed sponges.

199x297mm (300 x 300 DPI)

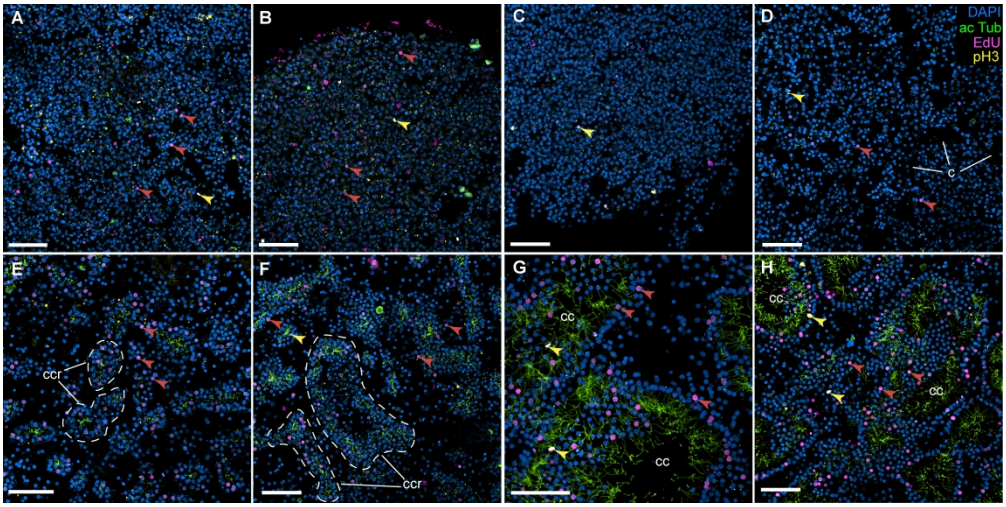

Fig. 4. Cell proliferation during the process of cell reaggregation and sponge reconstruction in Halisarca dujardinii. A – primary multicellular aggregate (1 day post-dissociation, dpd). B – early-staged primmorph (2 dpd). C – true primmorph (4 dpd). D – primmorph with developing aquiferous system, early stages (9 dpd). E – primmorph with developing aquiferous system, intermediate stages system (11 dpd). F – primmorph with developing aquiferous system, late stages (11 dpd). G – primmorph with oscular tube rudiments (22 dpd). H – reconstructed sponge (19 dpd). Each image is a maximum intensity projection, obtained from 22 μm (A) or 15 μm (B-H) Z-stack. Red arrowheads marks EdU-positive nuclei of DNA-synthesizing cells, yellow arrowheads – pH3-positive nuclei of mitotic cells. c – cavities of developing aquiferous system, cc – choanocyte chambers, ccr – rudiments of choanocyte chamber. Blue – DAPI, 4',6-diamidino-2-phenylindole, green – acetylated α-tubulin, magenta – EdU, 5-ethynyl-2′- deoxyuridine, yellow – phosphorylated histone3. Scale bar: 50 μm.

297x148mm (300 x 300 DPI)

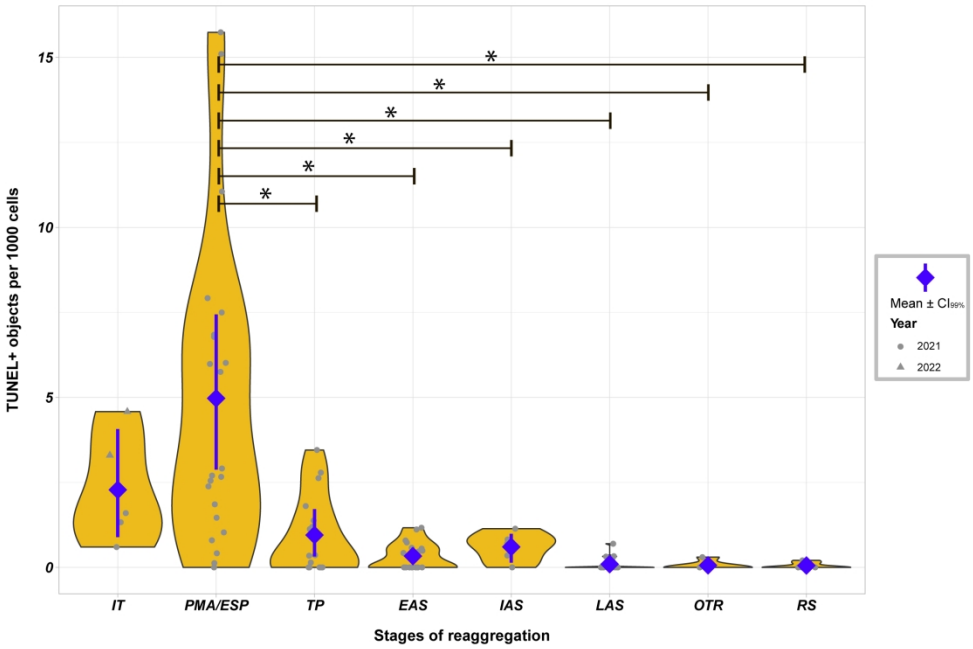

Fig. 5. Quantitative analysis of cell death in intact tissues and at the main stages of cell reaggregation process in Halisarca dujardinii. Asterisk – significant with p-values<0.01. IT – intact tissues, PMA – primary multicellular aggregates, ESP – early-staged primmorphs, TP – true primmorphs, EAS – primmorphs with developing aquiferous system, early stages; IAS – primmorphs with developing aquiferous system, intermediate stages; LAS – primmorphs with developing aquiferous system, late stages; OTR – primmorphs with oscular tube rudiments; RS – reconstructed sponges.

210x142mm (300 x 300 DPI)

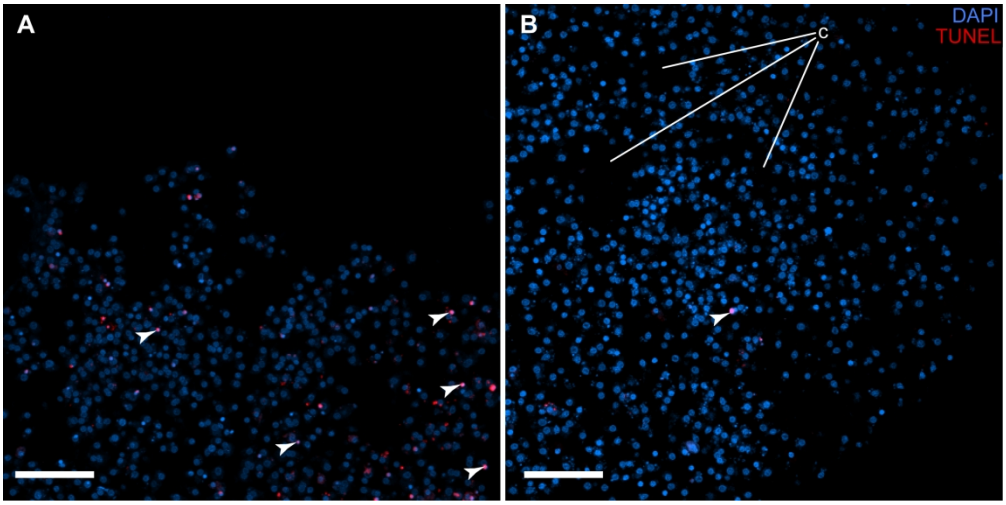

Fig. 6. Cell death during cell reaggregation in Halisarca dujardinii. A – numerous TUNEL+ objects in primary multicellular aggregate/early-staged primmorph (1 day post-dissociation, dpd); image is a maximum intensity projection (MIP), obtained from 25 μm Z-stack. B – single TUNEL+ nucleus in primmorph with developing aquiferous system, early stages (5 dpd) image is a MIP, obtained from 15 μm Z-stack. Blue – DAPI, 4',6-diamidino-2-phenylindole, red – TUNEL, terminal deoxynucleotidyl transferase dUTP nick end labeling. Scale bar: A, B – 50 μm.

210x104mm (300 x 300 DPI)

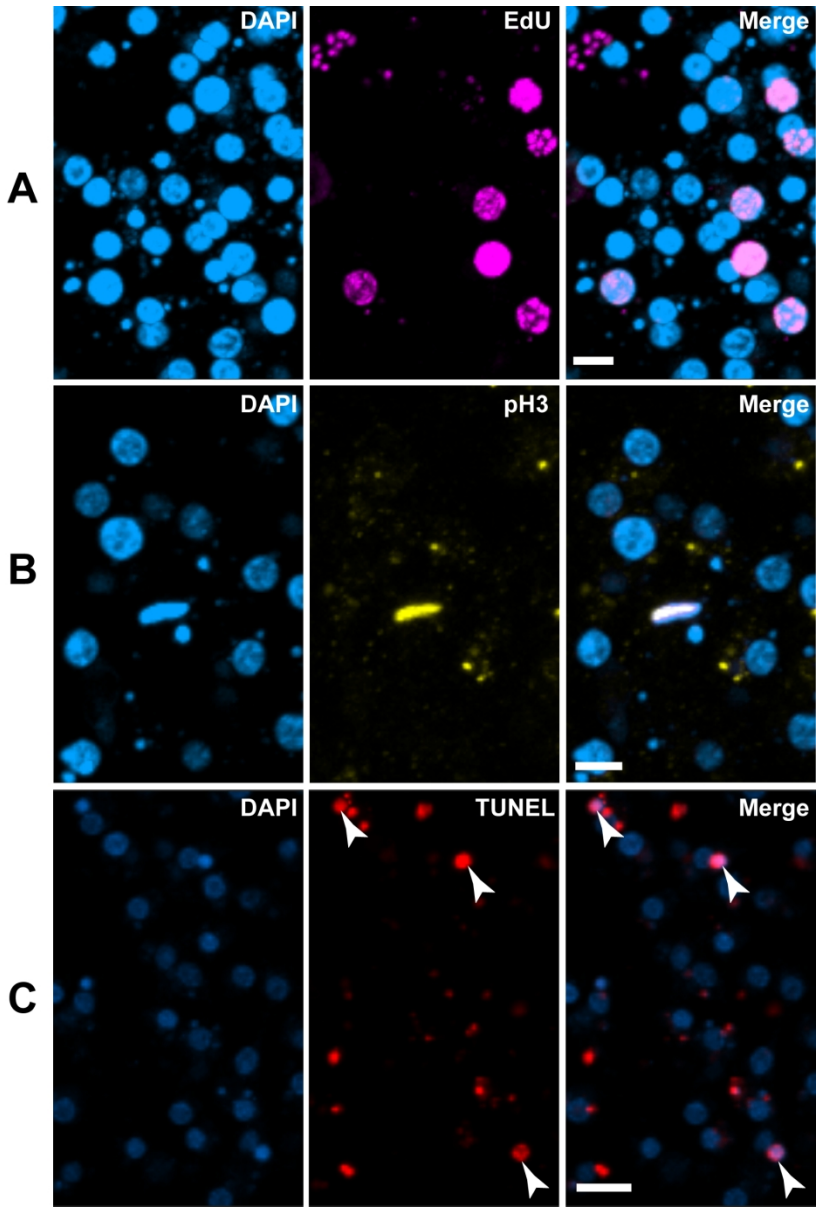

144x210mm (300 x 300 DPI)

Table S1. Number of aggregates at each stage of reaggregation used for proliferation studies.

Stage	Year	Individual	EdU incubation period, hpd	Number of aggregates
PMA				
	2019	Hd7 2019	0-24	4
	2020	Hd13 2020	0-24	6
	2020	Hd11 2020	0-24	3
	2020	Hd14 2020	0-24	8
		Total		***21***
ESP				
	2017	Hd4 2017	24-48	5
	2017	Hd5 2017	24-48	4
	2017	Hd6 2017	24-48	5
	2017	Hd7 2017	24-48	4
	2017	Hd8 2017	24-48	5
	2017	Hd9 2017	24-48	3
	2019	Hd6 2019	24-48	5
	2019	Hd7 2019	24-48	5
	2019	Hd15 2019	24-48	3
		Total		***39***
TP				
	2019	Hd6 2019	72-96	5
	2019	Hd7 2019	72-96	5
	2019	Hd14 2019	72-96	3
		Total		***13***
EAS				
	2017	Hd7 2017	120-144	5
	2017	Hd8 2017	120-144	5
	2017	Hd9 2017	120-144	5
	2019	Hd17 2019	72-96	9
	2019	Hd9 2019	144-168	5
	2020	Hd14 2020	144-168	6
	2020	Hd15 2020	120-144	5
	2020	Hd5 2020	192-216	5
		Total		***45***
IAS				
	2017	Hd5 2017	216-240	4
	2017	Hd7 2017	192-216	5
	2017	Hd8 2017	192-216	5
	2017	Hd9 2017	192-216	6
	2019	Hd15 2019	144-168	12
	2019	Hd17 2019	144-168	10
	2020	Hd8 2020	192-216	5
	2020	Hd7 2020	240-264	5
		Total		***52***

Stage	Year	Individual	EdU incubation period, hpd	Number of aggregates
LAS				
	2017	Hd8 2017	312-336	5
	2019	Hd15 2019	216-240	4
	2019	Hd17 2019	216-240	9
	2019	Hd15 2019	288-312	5
	2020	Hd12 2020	240-264	6
	2020	Hd8 2020	288-312	5
	2020	Hd11 2020	240-264	6
		Total		***40***
OTR				
	2020	Hd10 2020	432-456	4
	2020	Hd11 2020	432-456	5
	2020	Hd9 2020	528-552	5
	2021	Hd1 2021	504-528	7
		Total		***21***
RS				
	2020	Hd10 2020	432-456	9
	2021	Hd1 2021	624-648	6
		Total		***15***

PMA – primary multicellular aggregates, **ESP** – early-staged primmorphs, **TP** – true primmorphs, **EAS** – developing primmorphs with early aquiferous system, **IAS** – developing primmorphs with intermediate aquiferous system, **LAS** – developing primmorphs with late aquiferous system, **OTR** – developing primmorphs with oscular tube rudiments, **RS** – reconstructed sponges, **hpd** – hours post dissociation.

Table S2. Number of aggregates at each stage of reaggregation used for apoptosis studies.

Stage	Year	Individual	Age of aggregates, hpd	Number of aggregates
ESP				
	2021	Hd3	24	5
	2021	Hd4	24	7
	2021	Hd5	24	4
	2021	Hd6	24	7
		Total		***23***
TP				
	2021	Hd1	72	4
	2021	Hd2	72	6
	2021	Hd3	72	6
		Total		***16***
EAS				
	2021	Hd1	120	7
	2021	Hd2	120	6
	2021	Hd3	120	6
		Total		***19***
IAS				
	2021	Hd2	168	5
		Total		***5***
LAS				
	2021	Hd3	240	5
	2021	Hd1	336	5
	2021	Hd3	336	6
		Total		***16***
OTR				
	2021	Hd1	624	5
		Total		***5***
RS				
	2021	Hd1	456	6
		Total		***6***

ESP – early-staged primmorphs, **TP** – true primmorphs, **EAS** – developing primmorphs with early aquiferous system, **IAS** – developing primmorphs with intermediate aquiferous system, **LAS** – developing primmorphs with late aquiferous system, **OTR** – developing primmorphs with oscular tube rudiments, **RS** – reconstructed sponges, **hpd** – hours post dissociation.